Properties of Phased Arrays*

WILHELM H. VON AULOCK†, ASSOCIATE MEMBER, IRE

Summary—**This paper discusses in some detail the scanning properties of planar and linear phased arrays consisting of a large number of equispaced radiators, either omnidirectional or directive. Assuming that a suitable beam shape and sidelobe level in the broadside direction have been attained, it is shown how scanning of the array through introduction of a phase delay into the wave front distorts this pattern and introduces new sidelobes. The study uses contour maps of the antenna pattern in "sin θ-space," which is a projection of the unit sphere on the plane of the array. In this space the antenna pattern remains invariant with scan angle and merely undergoes a translation proportional to the phase delay between adjacent radiators. Using a parallel projection of the unit sphere onto the plane of the array, the actual antenna patterns are then readily obtained in conventional spherical coordinates. This method also permits ready evaluation of the influence of the directivity of the radiating elements, including a slight shift of the beam maximum with respect to that of an array of isotropic radiators. Furthermore, a pictorial representation of the coverage of a tilted planar array of given scanning properties can be obtained in terms of an earth-fixed coordinate system. Finally, it is shown how the beam-pointing error in a phased array is related to systematic errors in the phase delay.**

I. Introduction

MECHANICALLY scanned antennas were employed almost exclusively in the radar systems of World War II and are still being used in the majority of all operational radar systems. However, new requirements for radar systems, including rigidity and shock resistance of the antenna structure, volumetric rapid scanning of large antennas, and avoidance of any mechanical motion in the radar system, have led to an ever-increasing interest in electrically scanned antennas in which the antenna stays fixed in space and the radar beam is moved by introducing a phase delay into the radiated wave front. Such an antenna is called, briefly, a "phased array." Its properties are well understood and readily amenable to numerical and graphic analysis.

Although the purpose of a two-dimensional phased array is the same as that of a parabolic reflector in a two-gimbal mount, namely, to scan a radar beam, the characteristics of these two antennas have some fundamental differences, thus making it impossible simply to substitute one for the other in an existing radar system. Phased arrays can provide scanning patterns and scanning rates which are impossible to attain with mechanically scanned antennas. Conversely, a parabolic reflector can be turned and tilted to radiate an identical antenna pattern toward every point in a hemisphere, a task which is inherently impossible with a planar phased array. Furthermore, the scanning properties of a mechanically scanned antenna are readily described in a spherical coordinate system with its origin at the phase center of the antenna, whereas scanning of a phased array can be discussed more conveniently in a different coordinate system.

This paper presents a brief review of the scanning properties of phased arrays. The discussion is restricted to arrays of equispaced radiators located in a plane. Further, it is assumed that the variation of scan angle θ_s of these arrays,[1] hereinafter referred to as "scan sector," is large compared to the beamwidth. This assumption implies that the phased arrays consist of many radiating elements, possibly 50 to 100 radiators for a linear array and 2500 to 10,000 elements for two-dimensional arrays.

The introduction of a phase delay across the wave front radiating from an array has many consequences besides the obvious shift of the beam maximum.

1) The beamwidth increases as one scans away from broadside.
2) The beam shape changes slightly as one scans from broadside to moderate scan angles and is modified drastically for extreme scan angles close to 90° from broadside.
3) New sidelobes may appear at moderate to large scan angles.
4) The beam direction is slightly different from that computed by standard formulas.

All these effects are well understood. They have to be taken into account if one attempts to approximate the precise performance of a mechanically scanned antenna with a phased array. This discussion therefore deals with beam direction, beamwidth, and beam shape as functions of phase delay. Furthermore, the sensitivity of array performance to systematic excitation errors is reviewed.

As a result of this study, it is possible to state accuracy requirements for the phase delay of practical arrays. The capabilities and limitations of this type of scanning antenna will be apparent, and techniques for the design of such an array will emerge.

* Received by the IRE, October 30, 1959; revised manuscript received, March 4, 1960.

† Bell Telephone Labs., Inc., Whippany, N. J.

[1] The scan angle θ_s is defined as the angle between the array normal and the beam maximum.

The deterioration of array characteristics with random excitation errors has received considerable attention in the literature.[2–5] It is not to be discussed here because it is believed that systematic errors, rather than random errors, will limit the performance of multielement phased arrays.

Whereas mechanically scanned antennas are adequately described by giving two antenna patterns in orthogonal planes, this method of presentation is entirely unsatisfactory for a phased array whose pattern changes appreciably as the beam is scanned away from the array normal. To appreciate fully the characteristics of both linear and two-dimensional phased arrays, their patterns must be studied in a hemisphere rather than in two planes, and a pattern representation which permits the study of pattern changes as a function of scan angle must be found. Thus, the hemisphere, rather than two orthogonal planes, becomes the preferred space to be considered, and the planar, rather than the linear, phased array emerges as the principal object of this discussion. In particular, the two-dimensional array of isotropic radiators is used to show the variation of beam position, beam shape, beamwidth, and secondary beams with phase delay. Directive radiating elements will be introduced later to demonstrate their contribution to beam distortion, sidelobe level, and beam-pointing errors.

II. Two-Dimensional Phased Arrays of Isotropic Radiators

Consider a two-dimensional array of $M \cdot N$ equispaced isotropic radiators in the xy plane (Fig. 1). The radiators are excited by individual currents I_{mn} and provisions are made to introduce independent progressive phase delays in the x and y directions, so that the delay between adjacent radiators is ψ_x and ψ_x (radians), respectively. We want to examine the motion of the radar beam as a function of the phase delays and to study the variations of beam shape with the scan angle. Hence, we are not concerned with the classic problem of array theory which attempts to correlate the antenna pattern with the complex excitation coefficients I_{mn}, but we simply assume that this problem has been solved and that means exist to produce an acceptable amplitude pattern in the z direction normal to the array when all array elements are excited in phase ($\psi_x = \psi_y = 0$).

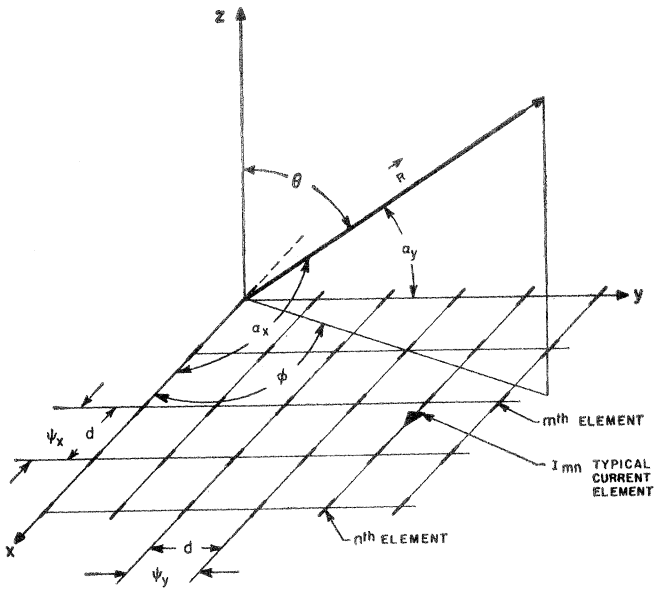

Fig. 1—Planar array of equispaced current elements.

A. The Antenna Pattern

The amplitude pattern of an array of isotropic radiators is given by[6]

$$S_a = \sum_{m=0}^{M-1} \sum_{n=0}^{N-1} |I_{mn}| e^{jd_r(m\tau_x + n\tau_y)}, \tag{1}$$

where

M, N = number of elements in x and y directions,

$|I_{mn}|$ = amplitude of excitation coefficient,

$d_r = 2\pi d/\lambda_0$ = spacing between radiating elements in radians,

λ_0 = wavelength in free space,

$\tau_x = \cos \alpha_x - \cos \alpha_{xs}$,

$\tau_y = \cos \alpha_y - \cos \alpha_{ys}$,

$\cos \alpha_x, \cos \alpha_y$ = direction cosines of radius vector specifying the point of observation,

$\cos \alpha_{xs}, \cos \alpha_{ys}$ = direction cosines of radius vector specifying beam maximum (scan direction).

The conventional pattern representation of this array uses a spherical coordinate system with azimuth and elevation angles ϕ and θ (Fig. 1). These angles are related to the direction cosines as follows:

$$\sin^2 \theta = \cos^2 \alpha_x + \cos^2 \alpha_y,$$

$$\tan \phi = \frac{\cos \alpha_y}{\cos \alpha_x}. \tag{2}$$

[2] L. A. Rondinelly, "Effects of random errors on the performance of antenna arrays of many elements," 1959 IRE National Convention Record, pt. 1, pp. 174–189.

[3] L. A. Kurtz and R. S. Elliot, "Systematic errors caused by the scanning of antenna arrays: phase shifters in the branch lines," IRE Trans. on Antennas and Propagation, vol. AP-4, pp. 619–627; October, 1956.

[4] D. K. Cheng, "Effect of arbitrary phase errors on the gain and beamwidth characteristics of radiation pattern," IRE Trans. on Antennas and Propagation, vol. AP-3, pp. 145–147; July, 1955.

[5] R. S. Elliot, "Mechanical and electrical tolerances for two-dimensional scanning antenna arrays," IRE Trans. on Antennas and Propagation, vol. AP-6, pp. 114–120; January, 1958.

[6] S. Silver, "Microwave Antenna Theory and Design," M.I.T. Rad. Lab. Ser., McGraw-Hill Book Co., Inc., New York, N. Y., vol. 12, pp. 104–106; 1949.

After fixing the direction of the beam maximum by specifying α_{xs} and α_{ys} and computing θ_s and ϕ_s from (2), one selects a plane $\phi=$const and computes the pattern

$$S_a = f(\theta) \qquad (\theta_s, \phi_s, \phi = \text{const}).$$

Similarly, one may compute the pattern

$$S_a = f(\phi) \qquad (\theta_s, \phi_s, \theta = \text{const}).$$

Clearly, this pattern representation has two disadvantages.

1) The pattern depends on the position of the beam maximum θ_s, ϕ_s.
2) The pattern representation is valid only for one particular plane ($\phi=$const) or conical surface ($\theta=$const). Hence, a complete representation of the antenna pattern in the hemisphere requires many curves for many different planes.

Both these difficulties can be overcome by using the differences of direction cosines τ_x and τ_y as variables and plotting a contour map of the amplitude pattern,

$$f(\tau_x, \tau_y) - S_a = 0 \qquad (S_a = \text{const}) \tag{3}$$

in direction cosine space.

Here we will assume that this particular contour is a circle for $M=N$ and an ellipse for $M\neq N$. It is interesting to note that this assumption is justified in the case of uniform illumination ($I_{mn}=I_0$). The amplitude pattern of an $M\cdot N$ array with uniform illumination[7] is given by

$$S_a = \frac{\sin \frac{1}{2}Md_r\tau_x}{M \sin \frac{1}{2}d_r\tau_x} \cdot \frac{\sin \frac{1}{2}Nd_r\tau_y}{N \sin \frac{1}{2}d_r\tau_y}. \tag{4}$$

The contour map of the main beam can be approximated by

$$S_a = \frac{\sin x}{x} \cdot \frac{\sin y}{y},$$
$$x = \tfrac{1}{2}Md_r\tau_x,$$
$$y = \tfrac{1}{2}Nd_r\tau_y. \tag{5}$$

This map is shown in Fig. 2. It is apparent that the contour is an almost perfect circle at the half-power point but approaches a square as S_a approaches zero. Hence, one may talk of a beam broadening in the diagonal. This beam broadening amounts to less than 2 per cent at the half-power point and may be neglected (Fig. 3). Thus, the half-power beamwidth of a uniformly illuminated square array ($M=N$) is given in τ space by

$$2\Delta\tau = \frac{C_0}{A/\lambda_0}, \tag{6}$$

where $C_0=0.888$ and $A=Nd$ (aperture).

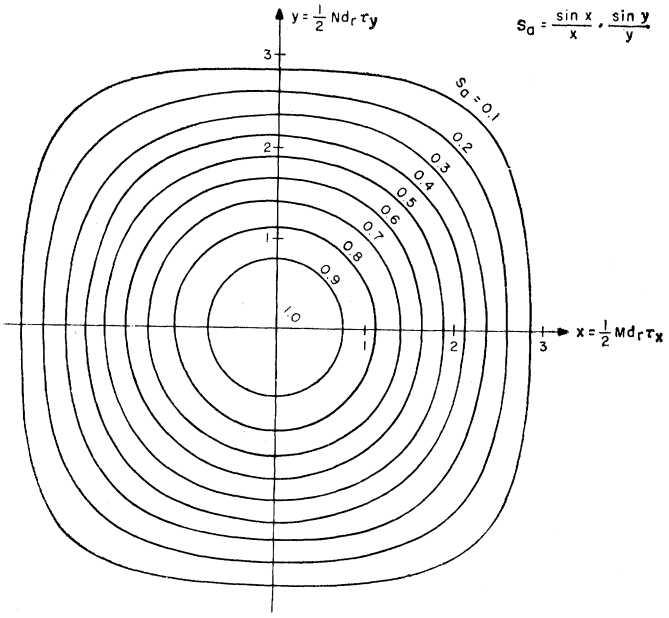

Fig. 2—Constant amplitude contours of the beam from a uniformly illuminated $M\cdot N$ planar array.

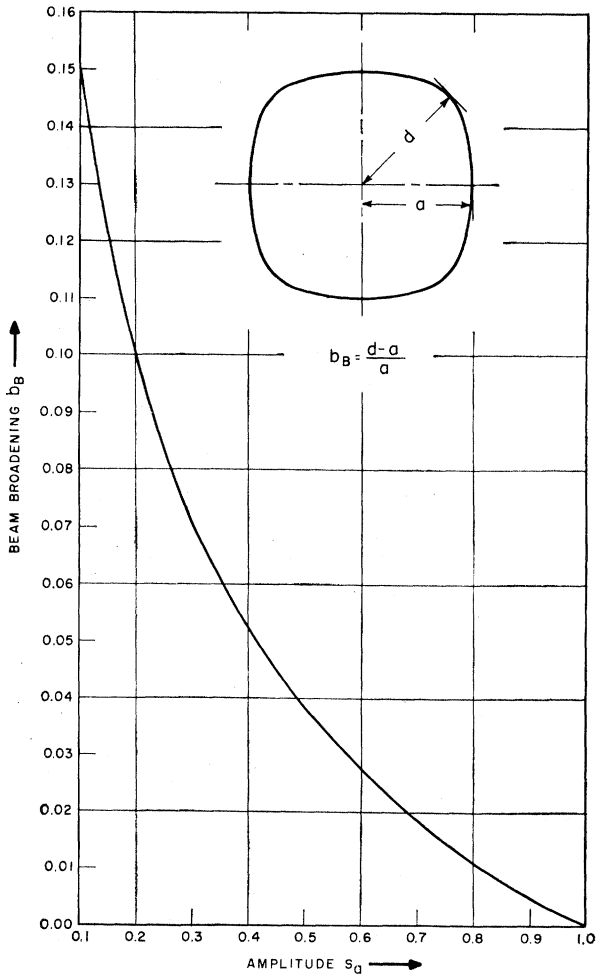

Fig. 3—Beam broadening of a uniformly illuminated planar array.

[7] J. D. Kraus, "Antennas," McGraw-Hill Book Co., Inc., New York, N. Y., ch. 4; 1950.

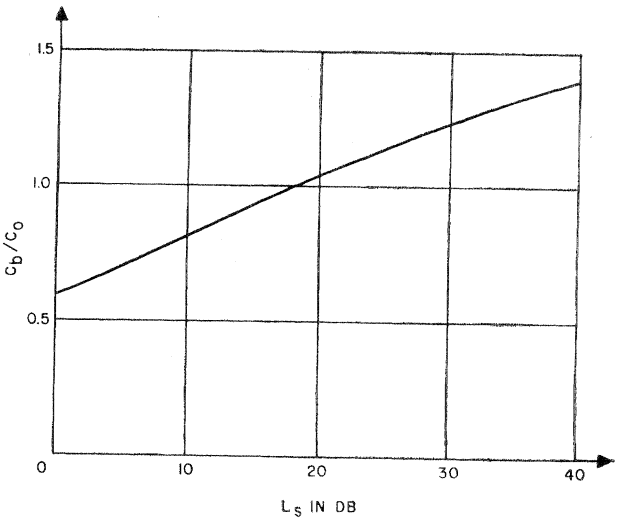

Fig. 4—Beamwidth of a Dolph-Tchebycheff array vs sidelobe level L_S relative to a uniformly illuminated array of equal aperture.

For a narrow beam array whose beam is oriented normal to the plane of the array, $2\Delta\tau$ can be interpreted directly as half-power beamwidth in radians. The beamwidth is related to the sidelobe level of the array in such a manner that the beam broadens when the excitation coefficients I_{mn} are tapered to satisfy specific sidelobe requirements. For a Dolph-Tchebycheff excitation function[8] (Fig. 4), the beamwidth can be expressed by

$$2\Delta\tau = \left(\frac{C_b}{C_0}\right)\left(\frac{C_0}{A/\lambda_0}\right), \tag{7}$$

where C_b/C_0 expresses the beam broadening with respect to uniform excitation and as a function of design sidelobe level. Note that a design sidelobe level of 40 db introduces a beam broadening of 41 per cent for a given aperture.

B. Scanning of the Beam

The direction of the beam maximum is a function of the two phase delays ψ_x and ψ_y so that the direction cosines are proportional to the respective phase delays:

$$\cos\alpha_{xs} = \frac{\psi_x}{d_r} \qquad \cos\alpha_{ys} = \frac{\psi_y}{d_r}. \tag{8}$$

This fundamental property of phased arrays makes it desirable to discuss pattern shape and beam motion in a coordinate system which has $\cos\alpha_x$ and $\cos\alpha_y$ for the two axes.

For ease of manipulation, let us then define a complex T plane with coordinates $\cos\alpha_x$ and $\cos\alpha_y$. This permits description of the point of observation by a single complex number T and locates the beam maximum in the T plane by another complex number, T_s.

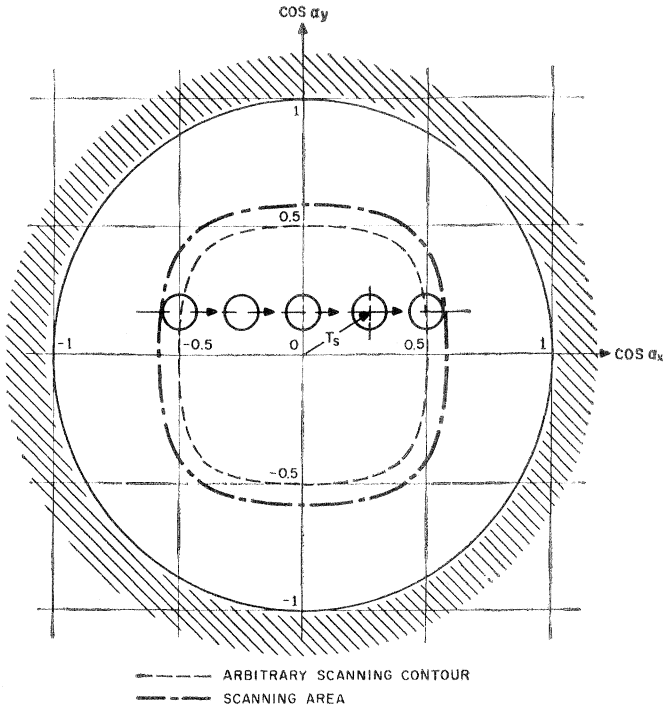

Fig. 5—Scanning in the complex T plane.

$$T = \cos\alpha_x + i\cos\alpha_y,$$

$$T_s = \cos\alpha_{xs} + i\cos\alpha_{ys} = \frac{\psi}{d_r}, \tag{9}$$

where $\psi = \psi_x + i\psi_y$ (phase delay).

Similarly, we can define a complex τ plane, which is suitable for contour maps of the amplitude pattern, by

$$\tau = T - T_s = \tau_x + i\tau_y. \tag{10}$$

The antenna pattern, which is a function of the complex variable τ, is invariant in the T plane. Scanning the antenna by introducing the complex phase delay $\psi = \psi_x + i\psi_y$ simply translates the pattern in space so that the pattern center moves to $T_s = \psi/d_r$ (Fig. 5). If the phase delay is chosen so that $|T_s| > 1$, the half-power contour moves outside of the unit circle and becomes imaginary, *i.e.*, unobservable.

Two definitions are helpful in discussing array properties:

The scanning contour—a closed curve in the T plane, traced by the beam maximum when the beam is scanned through the largest required deviations from the array normal (Fig. 5);

The scanning area—the area whose boundary is the outer envelope of all the half-power contours of the main beam when the beam is scanned along the scanning contour.

[8] L. B. Brown and G. A. Sharp, "Tschebyscheff Antenna Distribution, Beamwidth, and Gain Tables," Naval Ord. Lab., Corona, Calif., NAV-ORD Rept. No. 4629; 1958.

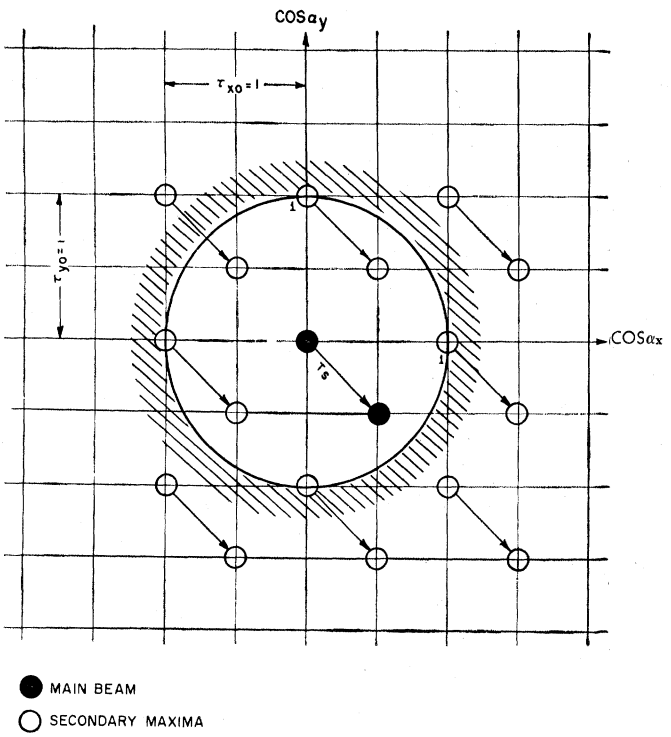

Fig. 6—Secondary maxima of a scanned array with one-wavelength element spacing.

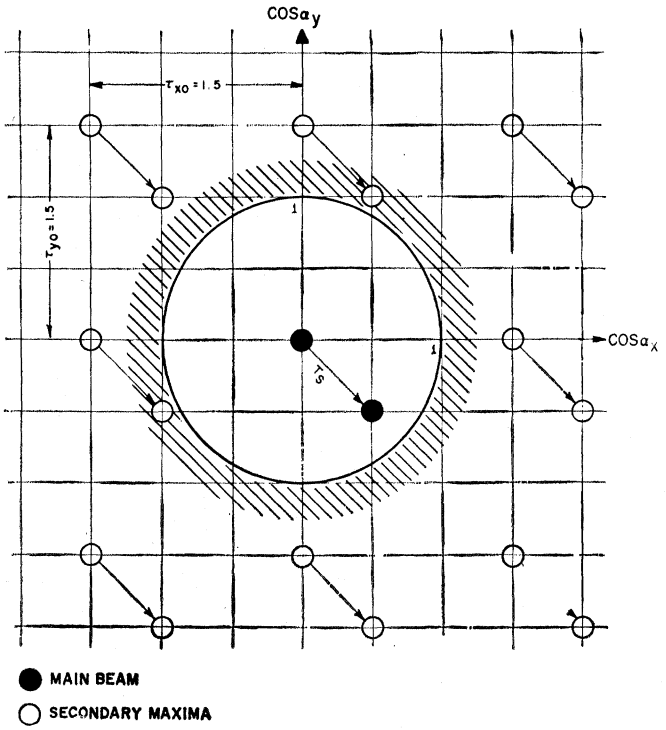

Fig. 7—Secondary maxima of a scanned array with two-thirds-wavelength element spacing.

C. Secondary Maxima

Let us now consider the effects of scanning on the beam pattern. The first is the occurrence of secondary maxima. An array of isotropic radiators has an infinite grid of these maxima spaced $\tau_{x0}=\tau_{y0}=\lambda_0/d$. The larger the element spacing, the closer the spacing of the maxima. Whenever the spacing is greater than $\lambda_0/2$, these maxima may become visible as they wander into the unit circle with each scanning of the array. If the elements in the array are spaced one free-space wavelength apart, the main beam and four endfire beams will be visible at zero scan angle (Fig. 6), and any scanning away from broadside will move a multiplicity of beams over the hemisphere. For example, if such an array is scanned by a phase delay $\psi=(1+i)\pi$, four beams will be seen on the circle $\theta=45°$. However, narrower spacing of the radiating elements (*e.g.*, $d=2\lambda_0/3$) will essentially suppress all secondary beams as long as $|T_s| \leqq \frac{1}{2}$ (Fig. 7).

Thus, the proper spacing of radiating elements is the first step in eliminating secondary beams in the array pattern. The second step is concerned with the proper choice of radiating elements (see Section IV).

D. Scanning of a Phased Array in a Spherical Coordinate System

All previous computations have been made in a coordinate system which was fixed with respect to the array, and it has been found that the antenna pattern remained invariant in direction cosine space (T plane). To examine the scanning characteristics of a phased array in its associated spherical coordinate system (Fig. 1), we have to project the orthogonal coordinates $\theta=$constant and $\phi=$constant onto the T plane. This projection permits immediate interpretation of the antenna pattern for any desired scan angle in terms of the spherical θ, ϕ system.

Expressing the complex direction cosine T in polar coordinates

$$T = \cos\alpha_x + i\cos\alpha_y = \sin\theta(\cos\phi + i\sin\phi),$$

$$T = \sin\theta e^{i\phi}, \tag{11}$$

immediately yields the desired projection which can be described as the parallel projection of the unit sphere on the equatorial plane (Fig. 8). Each circle $\sin\theta=$constant corresponds to two values of θ. Let us therefore define $0\leqq\theta\leqq\pi/2$ as the positive hemisphere and restrict our discussion to it.

E. Scanning Distortions in a Spherical Coordinate System

The resolution of a radar system is limited by the width of the radar beam. If this beamwidth depends on beam direction, then the resolution becomes a function of scan angle. To illustrate the magnitude of beam distortion in a phased array, consider a beam which is circular at the half-power points in T space. If this beam is scanned away from the array normal, it is then necessary to differentiate between two beamwidths in the θ and ϕ directions, respectively (Fig. 9). The reference

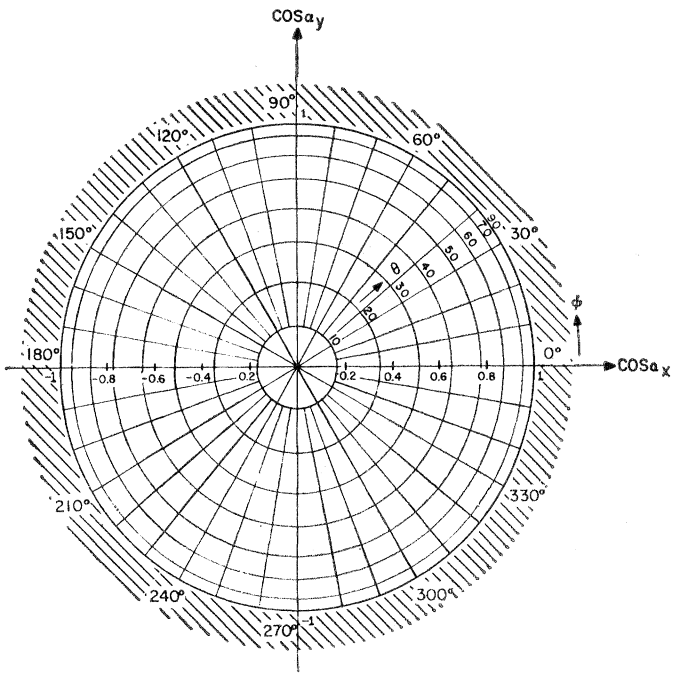

Fig. 8—Projection of unit sphere on T plane.

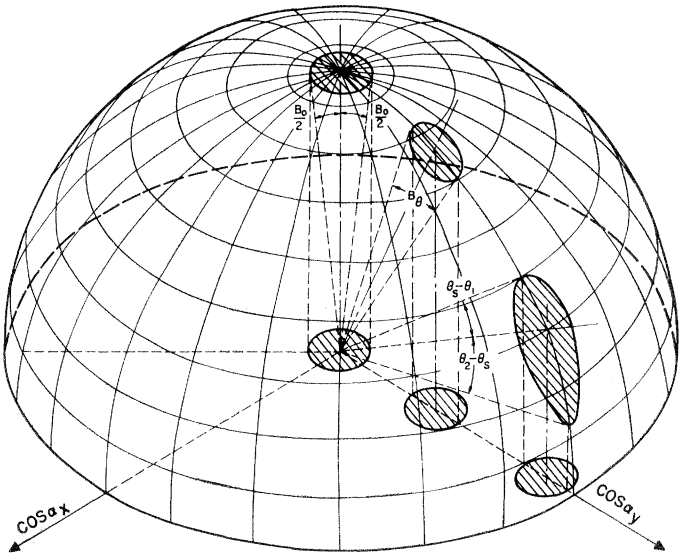

Fig. 9—Beamwidth and eccentricity of the scanned beam.

beamwidth is defined as [*cf.*, (7)]:

$$B_0 = 2 \sin^{-1} (\Delta\tau) \text{ (radians)}, \tag{12}$$

where $\Delta\tau = C_b\lambda_0/2A$. The beamwidth in the ϕ direction is constant and equal to B_0.

When the beam is directed away from the array normal, then the beamwidth B_θ in the θ direction is obtained from

$$2\Delta\tau = |T_2| - |T_1| = \sin\theta_2 - \sin\theta_1. \tag{13}$$

Thus

$$B_\theta = \theta_2 - \theta_1 = 2 \sin^{-1}\left(\frac{\Delta\tau}{\cos\frac{1}{2}(\theta_2 + \theta_1)}\right) \text{ (radians)}. \tag{14}$$

Eqs. (12) and (14) can be simplified for narrow-beam antennas in the usual manner, provided the scan angle $\theta_s \simeq (\theta_1+\theta_2)/2$ is not larger than, say, 45°:[9]

$$B_0 = 2\Delta\tau \text{ (radians)},$$

$$B_\theta = \frac{2\Delta\tau}{\cos\frac{1}{2}(\theta_2 + \theta_1)} \simeq \frac{B_0}{\cos\theta_s} \text{ (radians)}. \tag{15}$$

As the beam is scanned away from the array normal, it broadens in the θ direction. Hence, its contour at the half-power points changes gradually from a circle to an ellipse.

F. Beam Eccentricity

The assumption in (15) that $(\theta_2+\theta_1)/2 = \theta_s$ is inaccurate because the beam maximum is not centered between the two half-power points at θ_2 and θ_1. Thus, a beam eccentricity (Fig. 9) can be defined as

$$2e = \frac{(\theta_2 - \theta_s) - (\theta_s - \theta_1)}{(\theta_2 - \theta_s) + (\theta_s - \theta_1)}. \tag{16}$$

Use of a trigonometric identity and (15) as applied to $\theta_2 - \theta_s$ and $\theta_s - \theta_1$, the two "half" beams, in (16) yields

$$2e = \tan\tfrac{1}{4}(\theta_1 + \theta_2 + 2\theta_s) \tan\tfrac{1}{4}(\theta_2 - \theta_1). \tag{17}$$

As we are dealing with a second-order effect, (17) may be approximated by

$$e = \frac{B_\theta}{8} \tan\theta_s. \tag{18}$$

Note that the center of the beam moves relative to the contour by $(B_\theta^2/8) \tan\theta_s$ radians. For a narrow beam, this eccentricity is very small and may be neglected; however, for a broad beam, it can be appreciable.

Additional beam eccentricity is observed when the isotropic radiators are replaced by actual radiating elements which exhibit a particular element pattern. This effect is discussed in Section IV-A.

G. Endfire Beam

It has been shown that two phenomena limit the size of the practical scan sector,

1) the appearance of secondary maxima,
2) the broadening of the beam.

Both effects suggest maximum scan sectors of the order of $\pm 30°$ ($|T_s|_{\max} = \frac{1}{2}$). If an array with $2\lambda_0/3$ spacing is

[9] R. W. Bickmore, "A note on the effective aperture of electrically scanned arrays," IRE TRANS. ON ANTENNAS AND PROPAGATION, vol. AP-6, pp. 194–196; April, 1958.

scanned this far from its normal, maximum beam broadening in the θ direction is about 13 per cent and secondary maxima begin to appear at $\theta=90°$. It is this appearance of secondary maxima which requires a brief discussion of the beam shape close to $\theta=90°$.

The secondary maximum of an array of isotropic radiators appearing at $\theta=90°$ is, in effect, an endfire beam directed parallel to the array. Its beamwidth in the ϕ direction is equal to B_0, whereas its beamwidth $B_{\theta e}$ in the θ direction[10] is obtained from (13) by noting that $\theta_2=\pi/2$ and $\theta_1=(\pi/2)-B_{\theta e}$ and that $\Delta\tau$, rather than $2\Delta\tau$, applies (Fig. 10). We obtain the following approximation for a narrow-beam array:

$$B_{\theta e} = \sqrt{2\Delta\tau} = \sqrt{B_0} \text{ (radians)}. \tag{19}$$

Thus, an array with a reference beamwidth of 1° (0.017 radian) has an endfire beamwidth of $B_{\theta e}=7.5°$. Should the secondary maximum move just one-half beamwidth farther into the positive hemisphere, then its beamwidth increases by 41 per cent and is given by $\sqrt{2B_0}$. This substantial broadening of the endfire beam shows the importance of suppressing secondary maxima at $\theta=90°$ in a practical phased array through selection of appropriate radiating elements.

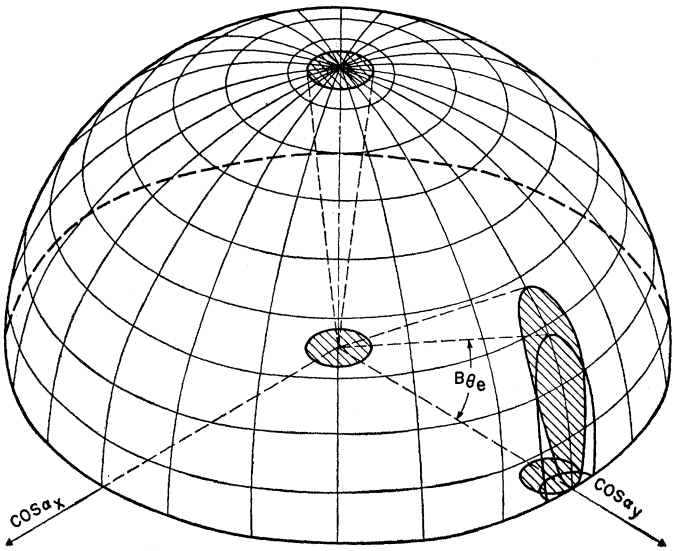

Fig. 10—Beam approaching endfire position.

III. Special Cases of Two-Dimensional Phased Arrays

A. The Linear Array

The discussion of two-dimensional phased arrays (see Section II) includes linear arrays as a special case. Putting $N=1$ in (1), we obtain the amplitude pattern of a linear array of isotropic radiators,

$$S_a = \sum_{m=0}^{M-1} |I_m| e^{jd_r m\tau_x}. \tag{20}$$

The contour map of the pattern of a linear array in direction cosine space is just a grid of lines parallel to the y axis (Fig. 11). In particular, the beamwidth between half-power points is again given by

$$2\Delta\tau_x = \frac{C_b}{A/\lambda_0}, \tag{7}$$

where $A=Md$ (aperture). Scanning of a linear array means moving a strip of width $2\Delta\tau_x$ across the T plane so that

$$T_{xs} = \sin\theta_s \cos\phi = \frac{\psi_x}{d_r}. \tag{21}$$

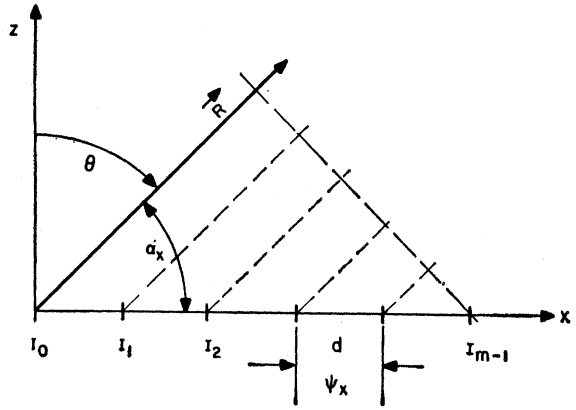

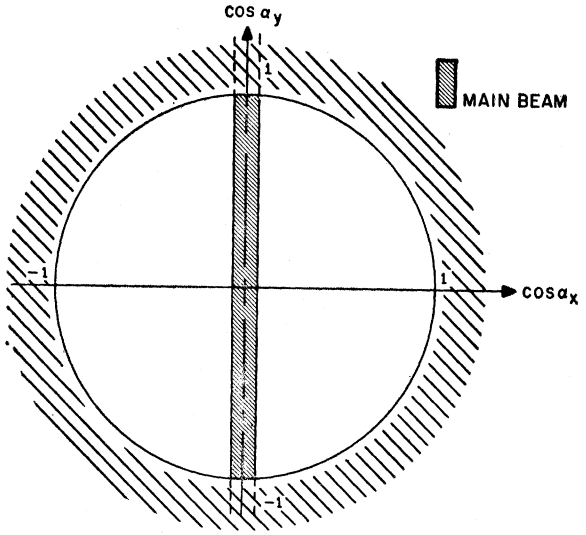

Fig. 11—Linear phased array.

[10] Consistent with our statement that we restrict our attention to the positive hemisphere, the endfire beamwidth is defined as $B_{\theta e}=(\pi/2)-\theta_1$.

If we again confine our attention to the positive hemisphere, then the actual beam of a linear array of isotropic radiators is a conical half shell. As the beam is scanned away from the array normal, the cone angle decreases and the cone contracts, much like an umbrella being folded, until at $\theta=90°$ it becomes a single endfire beam. The discussion of the endfire beam in Section II-G is readily adapted to the linear array and secondary maxima have the same spacing as before,

$$\tau_{x0}=\frac{\lambda_0}{d},$$

but have the appearance of strips in the T plane (Fig. 12). Their suppression through proper element spacing and suitably chosen radiating elements is guided by the considerations outlined in Section II-C and Section IV.

B. The Stacked Beam

A two-dimensional array of $M\cdot N$ radiators permits formation of a stacked beam (Fig. 13) by applying a multiplicity of fixed phase delays in the y direction. The stacked beam is then scanned by applying a variable phase delay in the x direction. There is a close similarity between the deformation of the stacked beam and of the beam of a linear array as a function of phase delay ψ_x. Here again, the aggregate of beams can be compared to a folding umbrella.

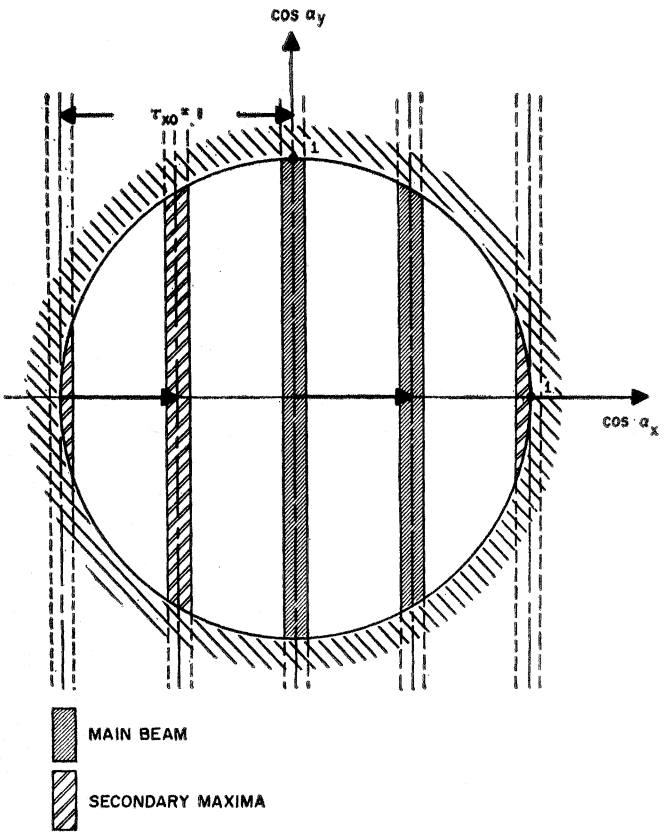

Fig. 12—Scanning of a linear array with one-wavelength element spacing.

C. The Four-Beam Cluster

In conventional radar systems, a four-beam cluster is employed to obtain monopulse information.[11] Such a four-beam cluster can readily be formed with a phased array by appropriate antenna feed structures with multiple outputs. In a phased array, the interpretation of the signal obtained from beams A, B, C, D (Fig. 14) must take into account the fact that the beam cluster cannot be rotated in the spherical coordinate system. Hence, the signals derived from $(A-C)$ and $(B-D)$ provide information relative to the θ direction when the cluster is scanned along the x axis ($\phi=0$). The same beam combination supplies information pertaining to the ϕ direction when the cluster is scanned along the y direction ($\phi=90°$). Similar reasoning applies to the difference signals $(A-B)$ and $(C-D)$.

[11] D. R. Rhodes, "Introduction to Monopulse," McGraw-Hill Book Co., Inc., New York, N. Y.; 1959.

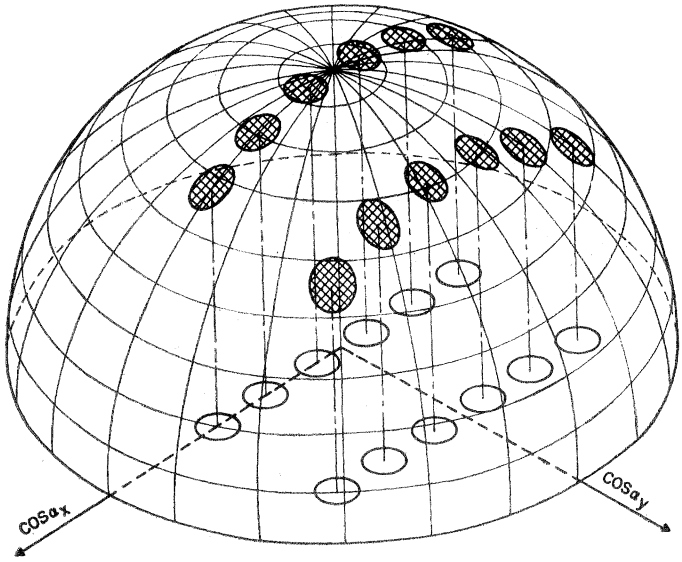

Fig. 13—Scanning of a stacked beam.

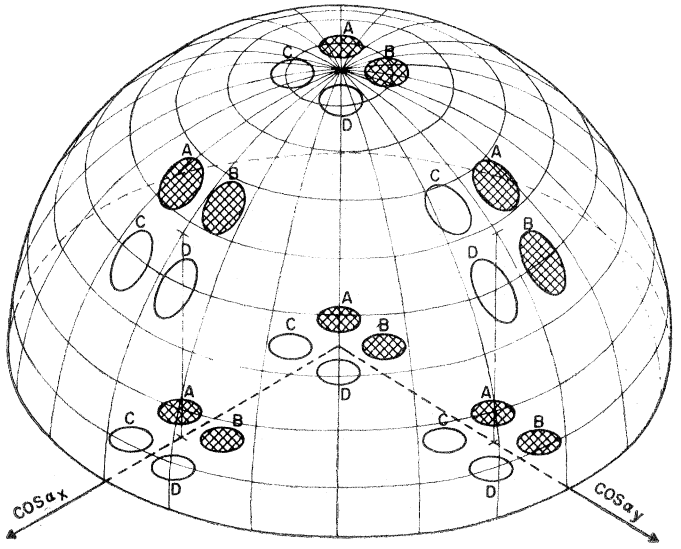

Fig. 14—Scanning of a 4-beam cluster.

IV. The Radiating Elements

In general, a phased array consists of identical directive radiators adjacent to a large reflecting ground plane. The pattern of such an array can be obtained by multiplying the pattern of the equivalent array of isotropic radiators S_a [see (1)] with the representative pattern of a single radiating element S_e, taking into account the effects of the ground plane and of mutual coupling between radiating elements. For the purpose of this discussion, let us assume that it is possible to find a single representative element pattern S_e. This implies that the array has many elements, thus providing a uniform environment for all elements except for a few at the very edge of the array. As the latter usually receive less illumination than the elements closer to the array center, their contribution to the over-all pattern is small.

Radiating elements assume many forms and shapes, such as dipoles, slots, open-end and tapered waveguides, polyrods, and helices. The free-space patterns of these radiators are reported in the literature and will not be discussed in detail. Rather, the requirements of an ideal radiating element will be stated, and the limitations of phased arrays will be discussed when the actual radiating elements fail to approximate this ideal.

First, the representative pattern S_e of the radiating element remains fixed in T space. It is, in effect, a window through which the scanned beam radiates into space. The ideal element factor S_e is therefore given by $S_e=1$ over the entire scanning area (Fig. 15) and $S_e \leqq L_s$ everywhere else (L_s is the highest acceptable sidelobe level).

Such an ideal pattern would permit scanning without introducing any additional distortion and would suppress all secondary maxima outside of the scanning area. In practical cases, the element pattern will drop from $S_e=1$ at $\theta=0$ to a prescribed value, such as $S_e=0.707$ (3 db), on the scanning contour. It is highly desirable to provide for a rapid decrease of S_e to 0 outside of the scanning area and for $S_e=0$ on the unit circle ($\theta=90°$). As an example, the pattern of a half-wave dipole at a distance of $\lambda_0/8$ from the ground plane is shown in Fig. 16.

Other radiating elements, such as horns or polyrods, can be designed to provide a better approximation to the ideal pattern. However, these radiators may not meet the fundamental requirement, namely, that their physical size permits close spacing of the radiating elements to suppress secondary maxima.

A detailed contour map of the representative pattern S_e of the array elements is required to determine the largest possible scanning contour (generally, the half-power contour) and the necessary element spacing. For example, the dipole pattern (Fig. 16) will permit scanning to 40.5° and 48.5° in x and y directions, respectively. This pattern has a sharp zero at $\theta=90°$. Hence, element spacing should be close to $\lambda_0/2$ to insure that secondary maxima stay outside the unit circle even at the largest practical scan angles.

If better radiating elements with steeper slopes of the pattern outside of the scanning area are available, the secondary maxima can be spaced closer to the main beam, thus permitting wider spacing of the radiating elements with attendant savings in hardware and circuitry. The theoretical maximum for element spacing is obtained from

$$\frac{\lambda_0}{d} = 2(\sin\theta_s + \Delta\tau). \tag{22}$$

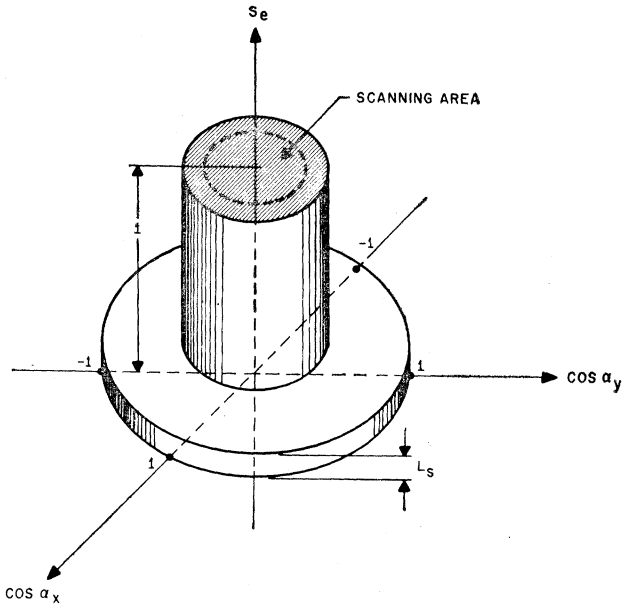

Fig. 15—Ideal element factor.

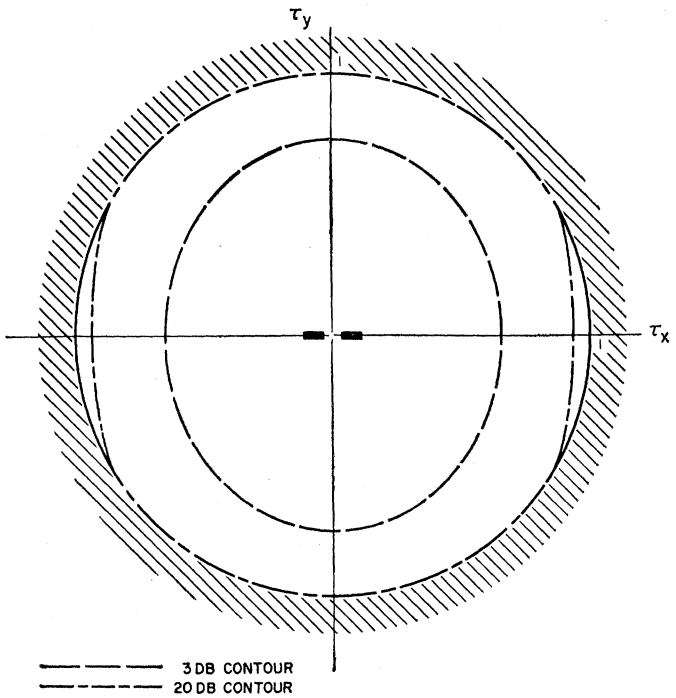

Fig. 16—Contour map of the pattern of a half-wave dipole located one-eighth wavelength above an infinite ground panel.

Hence, in special cases where only a small scan angle is desired, considerable savings can be realized by designing radiating elements which closely approximate the ideal pattern. If, for example, a $\frac{1}{2}$-degree beam were scanned $\pm 15°$, the radiating elements could be spaced $2\lambda_0$ apart, provided that the element factor S_e closely approximated Fig. 15.

For linear arrays, which are scanned in the x direction, the radiating elements determine the pattern shape in the y direction. Here, special requirements may have to be met, such as a squared cosecant pattern.

A. Correction for Beam Direction

The beam direction of an array of isotropic radiators was previously given [see (9)] as

$$\sin \theta_s e^{i\phi_s} = T_s = \frac{\psi}{d_r}.$$

It can be shown that the scan angle T_s must be corrected by a small quantity ΔT to account for the beam distortion (Fig. 17) which is introduced by the pattern S_e of the radiating elements. If S_e does not exhibit circular symmetry (*e.g.*, if S_e is a dipole pattern of the type shown in Fig. 16), then ΔT is a complex quantity; *i.e.*, it contains corrections for the θ and ϕ directions. If S_e is independent of ϕ or is circularly symmetric, the correction applies only to the θ direction. Restricting this study to the latter case, let us assume scanning along the real axis, where $T_s = \sin \theta_s$. The radiated amplitude pattern is given by

$$S = S_a S_e. \tag{23}$$

The correction for the beam maximum can be found by solving

$$\left.\frac{dS}{dT}\right|_{T=T_s-\Delta T} = 0 \tag{24}$$

for ΔT.[12] To simplify computation, the logarithmic patterns $F = \log S$, $F_a = \log S_a$, and $F_e = \log S_e$ are introduced. Then the first derivative of (23) is

$$F'(T) = F_a'(T - T_s) + F_e'(T), \tag{25}$$

where T_s is assumed constant. Expanding the right-hand side of (25) into a power series about T_s, we can solve (24) for ΔT,

$$\Delta T = \frac{F_e'(T_s)}{F_a''(0) + F_e''(T_s)} \simeq \frac{F_e'(T_s)}{F_a''(0)}. \tag{26}$$

In general, the curvature of the element pattern $F_e''(T_s)$ is much smaller than that of the array factor $F_a''(0)$ and may be neglected.

[12] The minus sign is chosen because the expected shift of the beam maximum is toward the array normal, *i.e.*, in the direction of decreasing T.

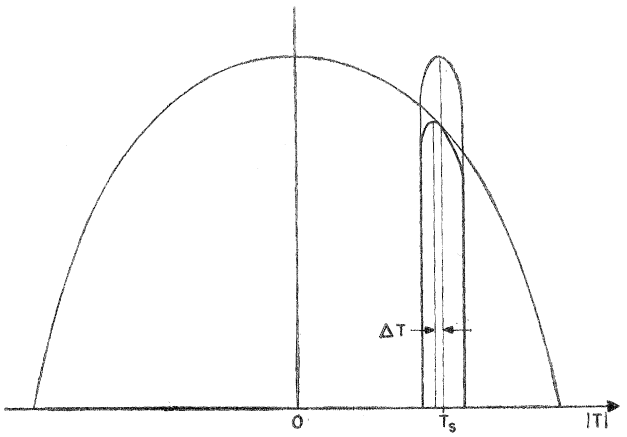

Fig. 17—Correction for beam direction of arrays consisting of directive radiators.

Thus, (26) permits ready evaluation of the correction factor ΔT from measured or computed antenna patterns. As an example, consider an array where both the array factor and the element pattern can be approximated by $S = (\sin x)/x$. Using the logarithmic pattern

$$F = \log \sin x - \log x, \tag{27}$$

where $x = Md_rT/2$, we find

$$\frac{dF}{dT} = -\frac{1}{T}(1 - x \cot x), \tag{28}$$

$$\frac{d^2F}{dT^2} = -\frac{1}{T^2}\left[\left(\frac{x}{\sin x}\right)^2 - 1\right]. \tag{29}$$

Using (29) to obtain the curvature of the array factor at $T = 0$ and introducing the beamwidth $2\Delta\tau_a$ from (6), we find that

$$F_a''(0) = -\frac{x^2}{3T^2} = -\frac{2.6}{(2\Delta\tau_a)^2}. \tag{30}$$

The quantity $F_a''(0)$ is inversely proportional to the square of the beamwidth. Using (28) to obtain the slope of the element factor at the half-power point and introducing the beamwidth $2\Delta\tau_e$, then

$$F_e'(T_s) = -\frac{1.5}{2\Delta\tau_e}. \tag{31}$$

The slope F_e' is inversely proportional to the beamwidth. Thus the maximum correction term $\Delta T_{\max}$, which applies to the maximum scan angle, can be expressed in terms of array and element beamwidth,

$$\Delta T_{\max} = 0.57\frac{(2\Delta\tau_a)^2}{2\Delta\tau_e}. \tag{32}$$

For a narrow-beam array, $\Delta T_{\max}$ is quite small and of the order of 10^{-3} to 10^{-4}. However, $\Delta T_{\max}$ increases with the square of the beamwidth and cannot be ignored for phased arrays which have a relatively broad beam.

Thus, the radiating elements may introduce beam distortion, sidelobes, and a small shift in beam direc-

tion. It may be concluded that proper design of radiating elements for phased arrays is of crucial importance to insure optimum performance. Despite substantial information on free-space patterns of a large variety of radiators, there is not yet enough information on the representative patterns of such elements as part of multielement phased arrays, and further investigations are needed.

V. Accuracy of Phased Arrays

In this study, the accuracy of a phased array is defined as the accuracy with which the direction of the beam maximum can be determined and reproduced by measuring and adjusting the phase delay between radiating elements. Using the conventional method of expressing beam position and its accuracy, it can be stated that the radiated beam maximum is determined by the spherical coordinates $\theta_s \pm \Delta\theta$ and $\phi_s \pm \Delta\phi$, with $\Delta\theta$ and $\Delta\phi$ designating the 2σ-values of a normal distribution around θ_s and ϕ_s. If the antenna were mechanically scanned around two or more orthogonal shafts, it would be reasonable to give values for $\Delta\theta$ and $\Delta\phi$ which would apply to scanning throughout the entire hemisphere. It is readily seen, however, that no such numbers $\Delta\theta$ and $\Delta\phi$ can exist for phased arrays. If it can be assumed that all necessary phase delays between zero and $\psi_{\max}$ can be produced with equal accuracy, then the two direction cosines $\cos \alpha_{xs}$ and $\cos \alpha_{ys}$ will have constant tolerances but $\Delta\theta$ and $\Delta\phi$ will depend upon the scan angle θ_s. From Section II-B, we obtain

$$d(\cos \alpha_{xs}) = \frac{1}{d_r} d\psi_x \qquad d(\cos \alpha_{ys}) = \frac{1}{d_r} d\psi_y.$$

These statements can be combined into a single equation in the complex T plane,

$$dT = \frac{1}{d_r} d\psi \tag{33}$$

A small change in complex phase shift is given by

$$d\psi = |\, d\psi \,| \, e^{i\epsilon}. \tag{34}$$

The differential dT can be expressed as an arc $d\gamma$ on unit sphere (Fig. 18) by rewriting it in spherical coordinates

$$dT = d(\sin \theta_s e^{i\phi_s}) = (\cos \theta_s d\theta + i \sin \theta_s d\phi) e^{i\phi_s}, \tag{35}$$

and computing $d\theta$ and $d\phi$

$$d\theta = \frac{\cos(\epsilon - \phi_s)}{d_r \cos \theta_s} \, |\, d\psi \,| \qquad d\phi = \frac{\sin(\epsilon - \phi_s)}{d_r \sin \theta_s} \, |\, d\psi \,|. \tag{36}$$

Then the tolerance for a phased array can be stated in terms of the angle $\Delta\gamma$:

$$\Delta\gamma \equiv \sqrt{(\Delta\theta)^2 + \sin^2 \theta_s (\Delta\phi)^2} = \frac{|\, \Delta\psi \,|}{d_r} \sqrt{1 + \tan^2 \theta_s \cos^2(\epsilon - \phi_s)}. \tag{37}$$

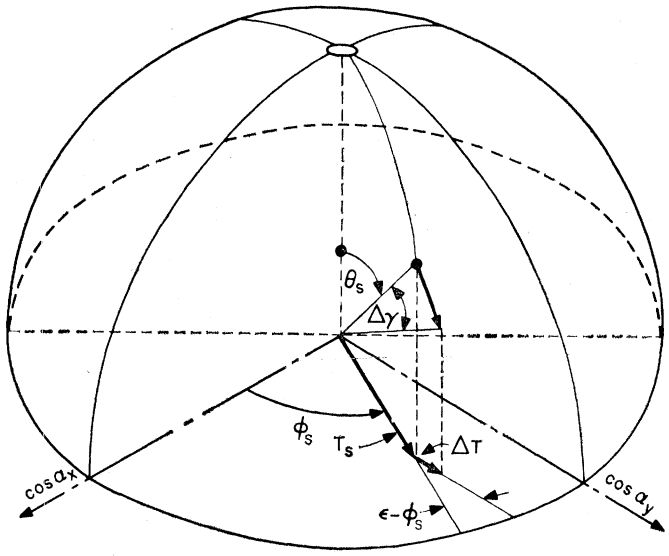

Fig. 18—Accuracy of phased arrays.

This result has the following significance:

1) Given a change in phase delay $\Delta\psi$ in the θ direction ($\epsilon = \phi_s$), the beam motion is proportional to $\Delta\psi$ in T space. Hence, for relatively small θ_s, the tolerance $\Delta\gamma$ is proportional to $\Delta\psi$. However, $\Delta\gamma$ increases with θ_s as $1/\cos \theta_s$ in exactly the same way as the beam broadens (Section II-E).
2) Given a change in phase delay $\Delta\psi$ in the ϕ direction ($\epsilon = \pi/2 + \phi_s$), the beam motion along the arc $\Delta\gamma$ is proportional to $\Delta\psi$ and hence independent of the scan angle θ_s.
3) The tolerance $\Delta\gamma$ is generally smaller than the tolerance $|\Delta\psi|$ because the constant of proportionality $1/d_r = \lambda_0/2\pi d$ is smaller than unity. For practical cases, $\frac{1}{2} > 1/d_r > \frac{1}{10}$; typically, $1/d_r = \frac{1}{4}$. This implies that a systematic error in phase delay of, say, $|\Delta\psi| = 1°$ produces a beam-direction accuracy of the order of $\frac{1}{4}$ degree, or less than 0.005 radian. This accuracy is not so good as that of modern, mechanically scanned antennas.

It is beyond the scope of this paper to discuss the design of accurate phased arrays, but we can point out here that the main problem appears to be the development of accurate methods to measure phase delay across the aperture of an array and of feedback and control circuitry which permits precise adjustment of phase shifters to the required values. Mechanical and electrical phase shifters are available for introducing the required phase delay.[13–15] Both appear to be capable of

[13] G. C. Southworth, "Principles and Applications of Waveguide Transmission," D. Van Nostrand Co., Inc., New York, N. Y., pp. 325–335; 1950.
[14] F. Reggia and E. G. Spencer, "A new technique in ferrite phase shifting for beam scanning of microwave antennas," Proc. IRE, vol. 45, pp. 1510–1517; November, 1957.
[15] F. E. Goodwin and H. R. Senf, "Volumetric scanning of a radar with ferrite phase shifters," Proc. IRE, vol. 47, pp. 453–454; April, 1959.

generating phase delays with an accuracy of $|\Delta\psi| = 1°$. These phase shifters may be used in parallel and series feed structures as well as in combinations of both (Fig. 19). In a series feed, all phase shifts ψ_i are equal to ψ; hence, programming is simple but errors in ψ show up directly as beam-direction errors. In a parallel feed, $\psi_{i+1} - \psi_i = \psi$; this implies that all ψ_i are different, requiring elaborate programming, but systematic errors in ψ_i have a tendency to compensate each other, at least partially. Furthermore, phase shifters in a parallel feed can be designed with considerably lower peak-power rating than phase shifters in a series feed. Thus, each of these feeds has its own peculiar problem with respect to systematic errors, frequency dispersion, complexity, and power-handling capability.

VI. Scanning of Phased Arrays in a Ground-Based Coordinate System

So far, the scanning characteristics of a phased array have been described in a spherical coordinate system which is fixed with respect to the array (Fig. 1). If the array were horizontal and oriented so that its x axis pointed north and its y axis pointed west, then the same coordinate system could be used as a ground-based system and the beam position and pattern shape could be interpreted immediately in terms of the angles θ and ϕ of a ground-based coordinate system. In general, this will not be the case; the array normal will be inclined by an angle θ_a from the vertical, and the plane of the array will not be horizontal. In fact, if the array were mounted on a ship or airplane, neither its x nor its y axis would normally be horizontal. Then the interpretation of beam direction in terms of a ground-based system would require a rotation of the array coordinate system through the Eulerian angles and a suitable coordinate transformation to find the beam direction and describe scanning distortions in a ground-based system.

This general case,[16] which is perfectly straightforward but somewhat involved and cumbersome, will not be treated here. But a simpler case, that of the ground-based tilted array, is given in some detail to show how its scanning performance can readily be studied by a parallel projection of a unit sphere belonging to the ground-based system on the T plane, which is fixed with respect to the array.

As an example, let the y axis of the array remain horizontal and point west. The array normal is then tilted forward through an angle θ_a so that the normal points north (Fig. 20). The array coordinates are primed to distinguish them from the coordinates x, y, z of the ground-based system. Rotating the array in the xy plane to obtain a principal direction (that of the z' axis) different from north does not introduce any complications and therefore will not be considered.

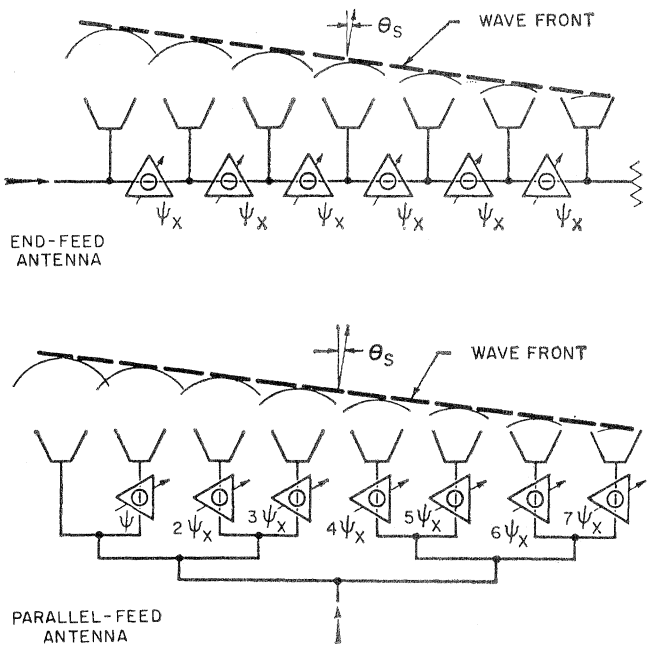

Fig. 19—Parallel-feed and series-feed antenna systems.

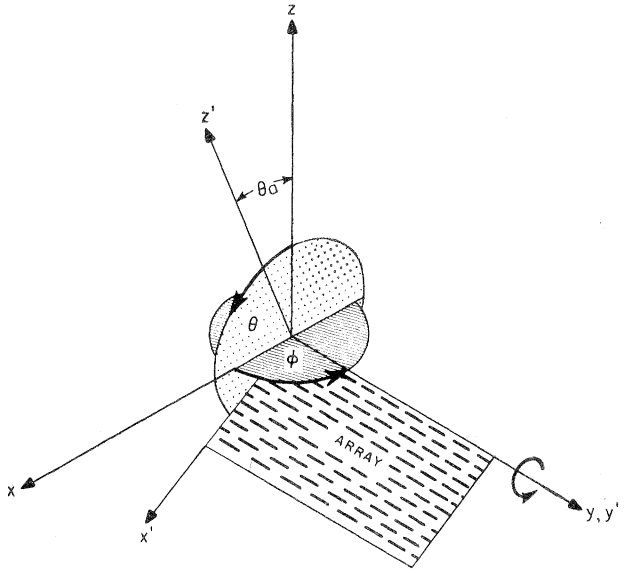

Fig. 20—Coordinate system of a tilted planar array.

Let $\vec{x}$ and $\vec{x}'$ be radius vectors in the ground-based and array coordinate systems, respectively:

$$\vec{x} = \begin{pmatrix} x \\ y \\ z \end{pmatrix} \qquad \vec{x}' = \begin{pmatrix} x' \\ y' \\ z' \end{pmatrix}.$$

Then $\vec{x}$ and $\vec{x}'$ are connected by the orthogonal transformations

$$\vec{x}' = \overleftrightarrow{A}\vec{x}, \tag{38}$$

$$\vec{x} = \overleftrightarrow{\bar{A}}\vec{x}'. \tag{39}$$

[16] H. Goldstein, "Classical Mechanics," Addison-Wesley Publishing Co., Inc., Reading, Mass., ch. 4; 1950.

where the rotation matrix $\overleftrightarrow{A}$ is given by

$$\overleftrightarrow{A} = \begin{pmatrix} \cos\theta_a & 0 & -\sin\theta_a \\ 0 & 1 & 0 \\ \sin\theta_a & 0 & \cos\theta_a \end{pmatrix}, \tag{40}$$

and $\overleftrightarrow{\tilde{A}}$ is the transpose of $\overleftrightarrow{A}$.

Two computations can be carried out, noting that on unit sphere

$$\begin{aligned} x &= \sin\theta\cos\phi &&= \cos\alpha_x, \\ y &= \sin\theta\sin\phi &&= \cos\alpha_y, \\ z &= \cos\theta &&= \cos\alpha_z, \\ x^2 + y^2 + z^2 &= x'^2 + y'^2 + z'^2 &&= 1. \end{aligned} \tag{41}$$

First, for a desired beam direction θ_s, ϕ_s in the ground-based coordinate system, the required phase shift is derived immediately from (38), (41), and (8),

$$\begin{aligned} \frac{\psi_x}{d_r} &= \cos\theta_a \sin\theta_s \cos\phi_s - \sin\theta_a \cos\theta_s, \\ \frac{\psi_y}{d_r} &= \sin\theta_s \sin\phi_s. \end{aligned} \tag{42}$$

Second, a mapping of the ground-based θ, ϕ system on the T plane is obtained by expanding (39),

$$\begin{aligned} \sin\theta\cos\phi &= x'\cos\theta_a + z'\sin\theta_a, \\ \sin\theta\sin\phi &= y', \\ \cos\theta &= -x'\sin\theta_a + z'\cos\theta_a. \end{aligned} \tag{43}$$

Using (41) and rearranging terms, the equations for lines of constant longitude ϕ and latitude θ are, respectively,

$$(y'\cot\phi - x'\cos\theta_a)^2 = (1 - x'^2 - y'^2)\sin^2\theta_a, \tag{44}$$

$$(\cos\theta + x'\sin\theta_a)^2 = (1 - x'^2 - y'^2)\cos^2\theta_a. \tag{45}$$

The latter can be rewritten to show that the lines of constant θ are ellipses with centers on the x' axis (see Fig. 21),

$$\frac{(x' + \sin\theta_a\cos\theta)^2}{(\cos\theta_a\sin\theta)^2} + \frac{y'^2}{\sin^2\theta} = 1. \tag{46}$$

The north pole ($\theta = 0$) is located at $x' = -\sin\theta_a$. We are interested only in that part of these ellipses which corresponds to the projection on the positive hemisphere. Hence, the intersection of these ellipses with the unit circle is located at $x' = -\cos\theta/\sin\theta_a$.

The lines $\phi = \text{const}$ appear as ellipses whose main axes are rotated with respect to the x' and y' directions. By rearranging terms in (44) and applying additional algebra, the equation of an ellipse in polar form ($x' = \rho\cos\epsilon$; $y' = \rho\sin\epsilon$) is obtained,

$$\frac{1}{\rho^2} = \frac{\cos^2(\epsilon - \epsilon_0)}{\sin^2\theta_a\sin^2\phi} + \sin^2(\epsilon - \epsilon_0), \tag{47}$$

in which $\cot\epsilon_0 = -\tan\phi\cos\theta_a$.

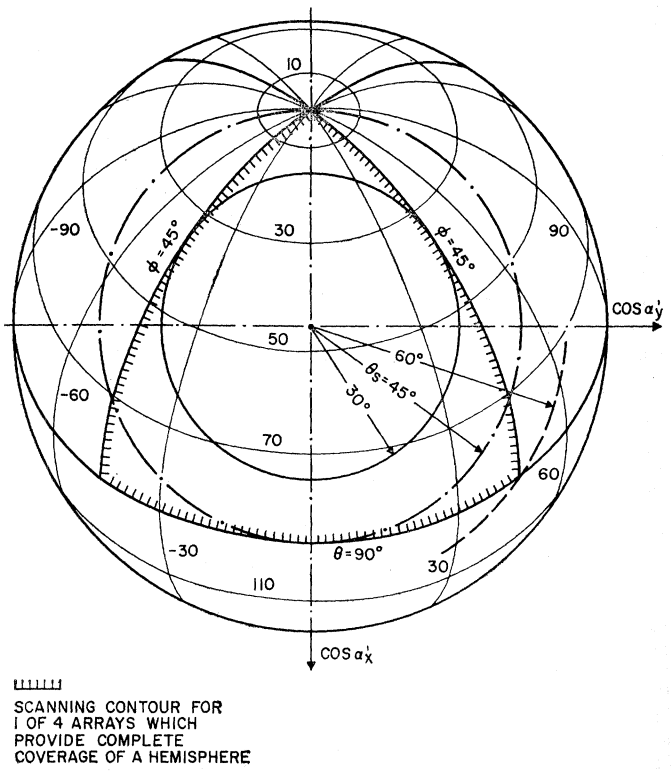

Fig. 21—Mapping of a ground-based spherical coordinate system onto the plane of an array whose normal is tilted 45° from the vertical.

The mapping given by (46) and (47) is very useful in determining the optimum tilt angle and scanning contour for a given scanning task. In general, a compromise will be needed between the scanning contour which gives the least beam distortion (see Sections II-E through II-G) and the scanning contour which provides the best coverage of the desired solid angle of the hemisphere. In the case of a phased array whose normal points straight up (Fig. 8), a circular scanning contour provides the best coverage. However, if complete coverage of a hemisphere is desired, then the scanning contours of several tilted arrays must be combined. If relatively large scanning distortions are permissible, then it is possible to cover the hemisphere with four phased arrays tilted 45° (Fig. 21). In this instance, a maximum scan angle of 45° would permit complete coverage to $\theta = 70°$, down to 20° elevation, whereas a maximum scan angle of 60° would be required to cover all points down to zero elevation. A circular scanning contour would provide considerable overlap at the north pole. This could be avoided by suitable programming of the phased arrays to obtain triangular scanning contours.

Acknowledgment

The author is indebted to W. E. Danielson, J. N. Hines, and I. Jacobs for many stimulating discussions and to R. S. McCarter for his critical reading of the manuscript. Miss J. Peterson and W. Pelish were most helpful in the preparation of the figures.